

## List of Revision

Our response to referee's comments are listed as **Red** in a marked pdf file.

(Comment 1)

*The backward trajectory of each dust storm was calculated using HYSPLIT. But there is no description of HYSPLIT and its advantages and disadvantages, except for a short sentence on P. 2. Many readers of NHESS are probably not familiar with HYSPLIT, a free downloadable model from the NOAA website, and will appreciate having some background information on the model.*

(Response 1)

For a broader audience, a brief introduction to "HYSPLIT" is necessary.

We have added five new sentences.

(Changes in manuscript 1)

**Lines 23-31, Page 2**

"The HYSPLIT has evolved from the earliest model in 1982 (Draxler and Taylor, 1982) from modelling long-range air parcel trajectories into simulations of pollutant transportation, dispersion, and deposition over global scales. As an open source, the HYSPLIT is available on the Web through the ARL READY system (<http://ready.arl.noaa.gov/HYSPLIT.php>), operated by the National Oceanic and Atmospheric Administration (NOAA) Air Resource Laboratory (ARL). The HYSPLIT model requires the meteorological input data, and it displays the analysis of the simulation outputs. One great advantage of using the Lagrangian HYSPLIT is that both forward and backward trajectories are available with local or global airflow patterns to interpret the transport of pollutants. The HYSPLIT model is continuously evolving to cope with turbulent mixing process and to incorporate higher temporal frequency data available from the meteorological data (Stein et al., 2015)."

(Comment 2) *The study mentions that the trajectories of air transport at altitudes of 1000, 1500, and 2000 m were traced and shows the trajectories in Fig. 1b. But after Fig. 1b, there is no more mention of these different altitudes. Are they involved in subsequent analysis?*

(Response 2)

Air transport at three different altitudes were handled independently.

We have added three new sentences.

(Changes in manuscript 2)

**Lines 1-5, Page 6**

"The HYSPLIT backward trajectories at different altitudes of 1000 m, 1500 m, and 2000 m were counted as individual path in the present study. They do not show a meaningful difference statistically, implying that atmospheric turbulent mixing was minimal. Such directional consistency for different altitudes of the HYSPLIT model might result from the relatively low and flat geographic conditions. For instance, both eastern China and western Korea are low in elevation, with bridging shallow Yellow Sea which extends 900 km in North-South directions and 700 km in East-West directions."

(Comment 3) *In the Introduction, the authors explain that ADS contain “surficial minerals of natural origin (e.g., weathered soils) as well as pollutants of anthropogenic origin such as black carbon, heavy metals, and sulfates.” But in the Discussion, the authors seem to identify the desertification of the Gobi and Taklamakan deserts as the main cause of the recent increase of ADS. Can pollutants of anthropogenic origin, such as from coal burning and industrial plants, be another reason for the increase?*

(Response 3)

Influence of anthropogenic particulate matters is now included.

We have added three new sentences.

(Changes in manuscript 3)

**Lines 21-25, Page 5**

“In addition to natural pedogenic enhancement, we cannot ignore the contribution of anthropogenic particulate matters supplied by fossil fuel combustion, coal burning and industrial plants. Although anthropogenic particulate matters represent only 5-30% of ADS volumetrically, they are harmful as they have a strong tendency to react with heavy metals preferentially. Considering on-going demand for the fossil-fuel combustion, it is reasonable to suggest that pollutants of anthropogenic origin are also responsible for the increase of ADS.”

(Comment 4) *The Discussion concentrates on the results from the four stations in South Korea. Are there studies from other countries such as Japan and Taiwan to support the findings of the study on the recent increase and seasonality of ADS?*

(Response 4)

Seasonality of Asian Dust Storm in other neighboring countries are included in discussion.

We have added two new sentences.

(Changes in manuscript 4)

**Lines 6-8, Page 5**

“Occurrence of more frequent ADS and its seasonality was also documented in neighboring countries including Japan and Taiwan (Yang, 2002; Watanabe et al, 2011; Chien et al., 2012; Kimura, 2012). Then, it can be understood that seasonal variation of ADS is a local, natural phenomenon in Eastern part of Asia.”

# Identification of Atmospheric Transport and Dispersion of Asian Dust Storms

Raegyung Ha<sup>1</sup>, Amarjargal Baatar<sup>2</sup>, Yongjae Yu<sup>2</sup>

<sup>1</sup>Department of Astronomy, Space Science, and Geology, Chungnam National University, Daejeon, 34134, Korea

5 <sup>2</sup>Department of Geology & Environmental Sciences, Chungnam National University, Daejeon, 34134, Korea

*Correspondence to:* Yongjae Yu (youngjaeyu@cnu.ac.kr)

**Abstract.** Backward trajectories of individual Asian dust storm (ADS) events were calculated using the hybrid single particle Lagrangian integrated trajectory (HYSPLIT) at four representative stations in Korea. A total of 743 ADS events and associated 2229 (endings of altitudes at 1000 m, 1500 m, and 2000 m per ADS event) backward trajectories from four  
10 stations were traced from January 2003 to August 2015. Regardless of the locations of the observed stations and the threshold time divide, recent increase of ADS occurrence rate was statistically significant in 99.9 % confidence limit. Winters and springs were high occurrence season for the ADS, while the ADS rarely occurred in summers. Angular distributions of dust transport indicated a dominance of northwesterly, as more than two-thirds of ADS events are azimuthally confined from 290°–340°. In addition, there is a tendency for stronger dust densities to be from the northwest.  
15 We found a strong inverse correlation between number of days with ADS events and cumulative dust density, indicating that the total amount of cumulative dust discharge was rather constant over time. If so, relatively shorter transport distance and more continental dust passage through Shandong peninsular would yield less but stronger dust concentration in shorter transport path.

## 1 Introduction

20 Asian dust storm (ADS) originates mostly in the Gobi and Taklamakan deserts, where high speed surface winds and intense dust storms soared dry, dense clouds of fine grained surface material. Once elevated, ADS spreads in the stratosphere, often reaches to the upper troposphere to form the dust devil (Yumimoto et al., 2009). These dusty clouds are then carried eastwards by prevailing westerly winds and pass over from China, Korea, Taiwan, Japan, and to the North Pacific in order (Hsu et al., 2012). These dusty clouds were eventually transported more than one full circuit around the globe in about two  
25 weeks (Uno et al., 2009). Such long range transport is possible as the dusty clouds are transported in atmospheric dusty layers (Tratt et al., 2001; Schepanski et al., 2009; Uno et al., 2009). It has been estimated that ADS contributes about 4 % of the global dust emission (Mahowald et al., 2010).

ADS contained surficial minerals of natural origin (e.g., weathered soils) as well as pollutants of anthropogenic origin such as black carbon, heavy metals, and sulfates (Guo et al., 2004; Hsu et al., 2004; Ramana et al. 2010). These pollutants have

impacts on climate variations as black carbons absorb solar irradiation (Jacobson 2001, 2012) whilst sulfates scatter solar radiation energy (Ramana et al. 2010). Deposition of anthropogenic pollutants also affects the human epidermal keratinocytes (Choi et al., 2011), dispersion of bacterial cells (Yamaguchi et al., 2012), and marine biogeochemical environment (Lin et al. 2007; Hsu et al. 2009). In addition, long range transport of ADS influences cardiovascular disease in  
5 Taiwan (Chen and Yang, 2005), cardiopulmonary emergence rate in Taiwan (Chan et al., 2008), worsening Asthma in Japan (Watanabe et al., 2011), daily mortality in Korea (Lee et al., 2013), and food toxicity in Japan (Kobayashi et al., 2015). Hence it is natural to raise public concern on the possible adverse effects of ADS in East Asia.

ADS influences air quality and the local ecological environment including vegetation and soil. It accelerated the process of desertification by increasing the rate of evaporation. Most of all, it has been observed that the frequency of ADS occurrence  
10 in East Asia increased as a result of desertification, over grazing and over farming, irrigation, and lack of precipitation in central Asia. Of course, it is also true that ADS is dependent on the synoptic climatic conditions such as cyclone activity, air temperature, and precipitation in source area (Natsagdorj et al. 2003; Qian et al. 2004; Hsu et al., 2013).

Over the past few decades, variation of ADS and its climate control has been explored (Natsagdorj et al. 2003; Qian et al. 2004; Kim et al. 2008; Lee et al., 2010; Zhao et al., 2010). For instance, Natsagdorj et al. (2003) compiled dust storms in  
15 Mongolia from 1937 to 1999, on the basis of observational data from 49 stations, found that annual mean number of days with dust storms were 20–37 days in the Gobi deserts and nearby arid area. Wang et al. (2005) defined three different types of dust storms and their characteristics in China, using data from 701 meteorological observation stations from 1954 to 2000. It should be highlighted that the number of ADS events increased by more than twice from 1960 to 2000 (Zhang et al. 2003; Wang et al. 2007, 2008).

20 Previous studies in Korea focused on the characteristic of dust particles and magnetic concentration of dust particles in ADS (Chun et al. 2001, 2008; Chung et al., 2003; Lee et al. 2006; Kim et al. 2008; Lee et al., 2013). In the present study, we trace the ADS trajectories using the hybrid single particle Lagrangian integrated trajectory (HYSPLIT) model (Draxler and Hess, 1998). The HYSPLIT has evolved from the earliest model in 1982 (Draxler and Taylor, 1982) from modelling long-range air  
25 parcel trajectories into simulations of pollutant transportation, dispersion, and deposition over global scales. As an open source, the HYSPLIT is available on the Web through the ARL READY system (<http://ready.arl.noaa.gov/HYSPLIT.php>), operated by the National Oceanic and Atmospheric Administration (NOAA) Air Resource Laboratory (ARL). The HYSPLIT model requires the meteorological input data, and it displays the analysis of the simulation outputs. One great  
30 advantage of using the Lagrangian HYSPLIT is that both forward and backward trajectories are available with local or global airflow patterns to interpret the transport of pollutants. The HYSPLIT model is continuously evolving to cope with turbulent mixing process and to incorporate higher temporal frequency data available from the meteorological data (Stein et al., 2015). The HYSPLIT model incorporates the meteorological data and vertical movement of atmospheric circulation to evaluate air parcel trajectories (Stein et al., 2015). Temporal and spatial variation of ADS allows a more comprehensive view of the dust generation and transport in East Asia. In particular, tracing the ADS trajectories in Korea is pivotal because Korea

is the first encountered out of source region of ADS on its westerly dominating dust transport. It is the purpose of this study to gain insight into how atmospheric transport, dispersion, and deposition of dusty particulates occurred in local scale.

## 2 Data

Korea Meteorological Administration (KMA) operates 28 local stations where each station records meteorological data including air pollution monitoring (<http://web.kma.go.kr/eng/>). In particular, KMA posted online real time insitu dust density measurements in major stations. Among 28 stations, we compiled data collected from four representative stations including Baekryeongdo (BR, 37°58'00" N, 124°38'00" E, western front), Kosan (KS, 33°17'00" N, 126°09'00" E, southern edge), Ulreungdo (UR, 37°03'00" N, 130°55'00" E, eastern tail), and Daejeon (DJ, 36°22'8" N, 127°20'49" E, central location) (Fig. 1a). To trace the ADS provenance source, the HYSPLIT model was displayed on ArcGIS program. Air mass trajectory analysis was carried out using the HYSPLIT model with global data assimilation system (Stein et al., 2015), at the time of ADS events (Fig. 1b). The trajectories of air transport at altitudes of 1000, 1500 and 2000 m were traced for 72 hours (Fig. 1b).

In general, dust density (PM10) less than 25  $\mu\text{g m}^{-3}$  is considered to be recommended by the World Health Organization. According to KMA, advisory warning is issued when the hourly averaged dust concentration ( $\rho_{dd}$ ) is expected to exceed 150  $\mu\text{g m}^{-3}$  for an hour. When the hourly averaged dust (PM10) concentration is expected to exceed 400  $\mu\text{g m}^{-3}$  for an hour, more significant danger warning is issued. In the present study, individual ADS event was accounted as the day with advisory warning. For each station, cumulative dust density ( $\rho_{cdd}$ ) was defined as  $\rho_{cdd} = \sum_{i=1}^{n_{ADS}} \rho_{dd}$  for days with ADS events ( $n_{ADS}$ ).

## 3 Result

Backward trajectories of individual ADS events were calculated using the HYSPLIT at four representative stations at BR, DJ, KS, and UR (Fig. 1a). The data archive includes a collection of HYSPLIT model since 2003 based on NCEP/NCAR reanalysis at the time of ADS events. Trajectories of dust transport at altitudes of 1000 m, 1500 m, and 2000 m were traced for 72 hours (Fig. 1b). A total of 743 ADS events and associated 2229 (three different endings of altitude per ADS event) backward trajectories from four stations were traced from January 2003 to August 2015 (Table 1, Supplementary Data 1–4). Then, ADS was classified into six transport path (Fig. 1b) on the basis of wind azimuth during the first 24 hours of each ADS event as N–NE (northerly 0° to northeasterly 45°), N–NW (northerly 360° to northwesterly 315°), W–NW (westerly 270° to northwesterly 315°), W–SW (westerly 270° to southwesterly 235°), S–SW (southerly 180° to southwesterly 235°), and S–SE (southerly 180° to southeasterly 135°) (Table 1).

Annual cycles of number of days each year with ADS events ( $n_{ADS}$ ) are displayed (Fig. 2). A modern data set with PM10 observation from 2003 to the present was combined with an old dataset without PM10 (Fig. 2). For the past 13 years, cumulative number of days with ADS events was 111 at BR, 220 at DJ, 257 at KS, and 155 at UR (Fig. 3a, Table 2). For

each station, annual and monthly variations of ( $n_{ADS}$ ) were similar with one another (Fig. 3b, c). However, it is interesting that ( $n_{ADS}$ ) of BR was systematically lower than that for other stations (Fig. 3b). For the past 13 years, the lowest frequency of ADS occurred in 2012 (Fig. 3b). Winters and springs were high occurrence season for the ADS, while the ADS rarely occurred in summers (Fig. 3c).

5 Temporal variations of dust density observed in each station were represented with time (Fig. 4 and Fig. 5). For each station, distribution of individual ( $\rho_{dd}$ ) was plotted as a function of time in lower panel (Fig. 4 and Fig. 5). In upper panels (Fig. 4 and Fig. 5), results were rearranged in boxplots where central box represents the interquartile of annual mean dust density and whisker lines are extending beyond the maximum and the minimum. For BR, a total of 111 ADS events from 2003 to 2015 showed mean dust densities ( $\rho_{mean}$ ) of  $424.7 \pm 341.1 \mu\text{g m}^{-3}$  (Fig. 4a, Table 2). On the other hand, values of ( $\rho_{mean}$ ) in  
10 other stations were smaller than those at BR (Table 2). For instance, DR, KS, and UR recorded mean dust densities of  $189.5 \pm 94.2 \mu\text{g m}^{-3}$  (Fig. 4b),  $190.7 \pm 62.3 \mu\text{g m}^{-3}$  (Fig. 4c), and  $188.3 \pm 55.7 \mu\text{g m}^{-3}$  (Fig. 4d), respectively. Danger warning issued days with ( $\rho_{dd}$ ) exceeding  $400 \mu\text{g m}^{-3}$  were 37 for BR (33.3 %), 5 for DJ (2.3 %), 7 for KS (2.7 %), and 3 for UR (1.9 %). Values of  $\rho_{dd}$  were tend to be larger over the spring seasons (Fig. 5).

On a log-log plot of ( $n_{ADS}$ ) versus ( $\rho_{dd}$ ), dust densities observed from BR plot in a line with a slope of -1.5, meaning that an  
15 order increase in dust density correlates with a 50-fold decrease in ADS occurrence (Fig. 6a). For UR, the slope of maximum asymptotic power fitting yielded -4.0, an order increase in dust density correlates with a four order decrease in ADS occurrence (Fig. 6a). Results for DJ and KS were confined within the trends of BR and UR (Fig. 6a). They were definitely not linear, but are tailed towards stronger values of dust densities for lower occurrence (Fig. 6a). We have constructed cumulative probability distribution functions for each station (Fig. 6b). Values of median dust density ( $\rho_{median}$ ) were 318.72  
20  $\mu\text{g m}^{-3}$  for BR, 162.13  $\mu\text{g m}^{-3}$  for DJ, 164.49  $\mu\text{g m}^{-3}$  for KS, and 171.62  $\mu\text{g m}^{-3}$  for UR (Fig. 6b).

Tracing the dust transport using the HYSPLIT was represented with angle histogram plot, which is a polar plot showing the distribution of prevailing wind in angle bins of 5 degrees (Fig. 7). For the past 13 years, spatial distribution of ADS events is prominently northwesterly (Fig. 7).

#### 4 Discussion

25 Cumulative number of days with ADS events ( $n_{ADS}$ ) for the past 13 years was 111 at BR, 220 at DJ, 257 at KS, and 155 at UR (Fig. 2, Fig. 3a, Table 2). Because of its shortest operation history, only the modern data are available in BR (Fig. 2a). More extended temporal coverages over 50 years of ADS events were available in DJ (Fig. 2b), KS (Fig. 2c), and UR (Fig. 2d). It is eye catching that the annual occurrence rate of ADS events has been increased recently (Fig. 2). For instance, annual mean occurrence rate of ADS in Daejeon was  $4.1 \pm 4.0$  from 1960 to 2000 and  $17.2 \pm 6.5$  from 2001 to 2015, which  
30 were significantly different ( $p = 7.611 \pm 10^{-7}$ ) each other according to the criteria of Welch's t-test with a significance of

99.9 % (Table 4). Regardless of the locations of the observed stations and the threshold time divide (either 1998 or 2001), recent increase of ADS events was statistically significant in 99.9 % confidence limit (Table 4).

Year to year variations (Fig. 3b) and month to month variations (Fig. 3c) of ADS events were compared. It is apparent that ADS is heavily concentrated in dry seasons, from February to June (Fig. 3c). The highest dust density occurred was 2371  $\mu\text{g m}^{-3}$  on April 8, 2006 at BR, 862  $\mu\text{g m}^{-3}$  on September 12, 2010 at DJ, 1342  $\mu\text{g m}^{-3}$  on April 2, 2007 at KS, and 440  $\mu\text{g m}^{-3}$  on April 02, 2007 at UR (Fig. 4 and Fig. 5). Occurrence of more frequent ADS and its seasonality was also documented in neighboring countries including Japan and Taiwan (Yang, 2002; Watanabe et al, 2011; Chien et al., 2012; Kimura, 2012). Then, it can be understood that seasonal variation of ADS is a local, natural phenomenon in Eastern part of Asia.

Several factors are known to be closely related with the occurrence and strength of dust storms including extinction of pastureland, abandoning cropland without vegetation cover, overexploitation of forests and shrubs, enhancement of mining activities, unregulated wild roads desertification, increase of human or factory transport, and decline of annual precipitation (Xuan et al., 2004; Aoki et al., 2005; Bian et al., 2011). Increase of desertification results in high dust emission from the places with less vegetation cover with dry and loose sandy soils in the Gobi and Taklamakan deserts (Laurent et al., 2005, 2006; Zhang et al., 2008). Recent increase of ADS events is contemporaneous to the increased desertification in the Gobi and Taklamakan deserts. For instance, numbers of the dusty days in the Gobi deserts have been almost tripled in recent years when compared to those in 1960's (Natsagdorj et al., 2003). In another occasion, it has been reported that sandy desertification in North China increased rapidly with mean annual areal expansion of 2460  $\text{km}^2$  (Zhang et al., 2008). In addition, decrease on the amount of soil moisture and increase of mean wind speed provide more frequent generations of dust storms (Natsagdorj et al. 2003). It should be highlighted that the highest frequency of ADS arose from the Gobi deserts, mostly in spring season due to the development of lower air temperature in winter season and high frequencies of cyclone activities (Qian et al., 2002). In addition to natural pedogenic enhancement, we cannot ignore the contribution of anthropogenic particulate matters supplied by fossil fuel combustion, coal burning and industrial plants. Although anthropogenic particulate matters represent only 5-30% of ADS volumetrically, they are harmful as they have a strong tendency to react with heavy metals preferentially. Considering on-going demand for the fossil-fuel combustion, it is reasonable to suggest that pollutants of anthropogenic origin are also responsible for the increase of ADS.

To evaluate the differences between the data sets observed from four different stations, a Kolmogorov–Smirnov test of a non-parametric and distribution free statistics was applied. When the value of P is insignificant (e.g.,  $P < 0.01$ ), we can reject the null hypothesis of no difference between the two data sets. According to the Kolmogorov–Smirnov test, data sets KS and UR are similar ( $P=0.7040$ ) and those between DJ and KS are somewhat similar ( $P=0.0280$ ) in 98 % confidence limit. Contrary to the initial impression based on the correlation between N and pdd (Fig. 6a) and that between N and pcdd (Fig. 6b), however, all other pairs of data sets are statistically different (Table 3). Angular distribution of dust transport indicates a dominance of northwesterly (Fig. 7). In fact, the prevailing ADS is from a narrow sector between  $290^\circ$  and  $340^\circ$  (Fig. 7). There is a tendency for stronger dust densities to be from the northwest (Fig. 7).

The HYSPLIT backward trajectories at different altitudes of 1000 m, 1500 m, and 2000 m were counted as individual path in the present study. They do not show a meaningful difference statistically, implying that atmospheric turbulent mixing was minimal. Such directional consistency for different altitudes of the HYSPLIT model might result from the relatively low and flat geographic conditions. For instance, both eastern China and western Korea are low in elevation, with bridging shallow Yellow Sea which extends 900 km in North-South directions and 700 km in East-West directions.

As ADS is a randomly occurring natural hazard, populations of individual ADS events ( $n_{ADS}$ ) should follow the exponential probability density distribution with the weaker dust density occurs more frequently (Fig. 6a). As anticipated,  $n_{ADS}$  versus  $\rho_{dd}$  displayed an inverse power relation in all four stations (Fig. 6a). But why did each station record a different power relation?

Thermodynamic equilibrium of wind-blown dust requires competing balance among uprising buoyancy, gravitational settlement, and flow resistant drag force. Strong inverse correlation between the number of days with ADS events ( $n_{ADS}$ ) and cumulative dust density ( $\rho_{cdd}$ ) implies that the total amount of cumulative dust discharge is rather constant over time. As a result of the nearly constant dust discharge, relatively shorter transport distance along with more continental dust passage through Shandong peninsular would yield less but stronger dust concentration in BR (Fig. 8a). In other words, longer settlement time intervals were required for DJ, KS, and UR (Fig. 8a), simply because they are located farther than BR from the dust sources (Fig. 1).

Mean dust density ( $\rho_{mean}$ ) was estimated by dividing the total amount of cumulative dust flux to the total number of ADS events ( $n_{ADS}$ ). In fact,  $\rho_{mean}$  is equivalent to the arithmetic mean of  $\rho_{dd}$  for each station. However, it is true that individual dust density distribution is far from being Gaussian or Log-Normal (Fig. 6b). Instead, median dust density ( $\rho_{median}$ ) estimated from the cumulative dust density distribution is useful to reflect individual dust density distribution. Regardless of distribution of natural hazards, the median is inherently more stable than the mean with respect to the uncertainty and will change less over time (e.g., Atkinson and Goda, 2011). Nonetheless, as far as the present study is concerned,  $\rho_{mean}$  and  $\rho_{median}$  can both reflect the mean dust densities as they are positively correlated (Fig. 8b).

*Author Contribution.* RH, AB, and YY carried out data compilation, statistical analysis and drafted the manuscript. RH and YY conceived of the study and participated in its design and coordination. RH and YY was in charge of the climatological interpretation. All authors read and approved the final manuscript.

*Acknowledgements.* This work was supported by This work was supported by the Polar Academic Program (PD1601), Korea Polar Research Institute, 2016. We thanks to Doohee Jeong, Hanul Kim, and Hoabin Hong for providing technical assistance in using scanning electron microscopy.

*Competing Interests.* The author declares that they have no conflict of interest.

## References

- Aoki, I., Kurosaki, Y., Osada, R., Sato, T., Kimura, F.: Dust storms generated by mesoscale cold fronts in the Tarim Basin, Northwest China., *Geophys. Res. Lett.*, 32, L06807, doi:10.1029/2004GL021776, 2006.
- Atkinson, G. and Goda K.: Effects of seismicity models and new ground motion prediction equations on seismic hazard assessment for four Canadian cities, *Bulletin of Seismological Society of America*, 101, 176–189, 2011.
- 5 Bian, H., Tie, X., Cao, J., Ying, Z., Han, S., Xue, Y.: Analysis of a severe dust storm event over China: Application of the WRF-Dust model, *Aerosol. Air Qual. Res.*, 11, 419–428, 2011
- Chan, C. C., Chuang, K. J., Chen, W. J., Chang, W. T., Lee, C. T., Peng, C. M.: Increasing cardiopulmonary emergency visits by long-range transported Asian Dust Storms in Taiwan, *Environ. Res.*, 106(3), 393–400, 2008.
- 10 Chen, Y. S., Yang, C. Y.: Effects of Asian Dust Storm events on daily hospital admissions for Cardiovascular disease in Taipei, Taiwan, *J. Toxicol. Env. Health*, 68, 1457–1464, 2005.
- Chien, L. C., Yang, C. H., Yu, H. L.: Estimated Effects of Asian Dust Storms on Spatiotemporal Distributions of Clinic Visits for Respiratory Diseases in Taipei Children (Taiwan), *Environ. Health Persp.*, 120, 8, 1215, 2012.**
- Choi, H., Shin, D. W., Kim, W., Doh, S. J., Lee, S. H., Noh, M.: Asian dust storm particles induce a broad toxicological transcriptional program in human epidermal keratinocytes, *Toxicol. Lett.*, 200, 92–99, 2011.
- 15 Chun, Y., Kim, J., Choi, J. C., Boo, K. O., Oh, S. N., Lee, M.: Characteristic number size distribution of aerosol during Asian dust episode in Korea, *Atmos. Environ.*, 35, 2715–2721, 2001.
- Chun, Y., Cho, H. K., Chung, H. S., Lee, M.: Historical records of Asian dust events (Hwangsa) in Korea, *Bulletin of American Meteorological Society*, 89, 823–827, 2008.
- 20 Chung, Y., Kim, H., Dulam, J., Harris, J.: On heavy dustfall observed with explosive sandstorms in Chongwon-Chonju, Korea in 2002, *Atmos. Environ.*, 37, 3425–3433, 2003.
- Draxler, R. D. and Hess, G. D.: An overview of the HYSPLIT\_x modelling system for trajectories, dispersion, and deposition, *Aust. Meteorol. Mag.*, 47, 295–308, 1998.
- Guo, J., Rahn, K. A., Zhuang, G.: A mechanism for the increase of pollution elements in dust storms in Beijing, *Atmos. Environ.*, 38, 855–862, 2004.
- 25 Hsu, S. C., Liu, S. C., Lin, C. Y., Hsu, R. T., Huang, Y. T., Chen, Y. W.: Metal compositions of PM10 and PM2.5 aerosols in Taipei during Spring, 2002, *Terr. Atmos. Ocean. Sci.*, 15(5), 925–948, 2004.
- Hsu, S. C., Liu, S. C., Arimoto, R., Liu, T. S., Huang, Y. T., Tsai, F., Lin, F. J., Kao, S. J.: Dust deposition to the East China Sea and its biogeochemical implications, *J. Geophys. Res.*, 114(D15), D15304, 10.1029/2008JD011223, 2009.
- 30 Hsu, S. C., Huh, C. A., Lin, C. Y., Chen, W. N., Mahowald, N. M., Liu, S. C., Chou, C. C. K., Liang, M. C., Tsai, C. J., Lin, F. J., Chen, J. P., Huang, Y. T.: Dust transport from non-East Asian sources to the North Pacific, *Geophys. Res. Lett.*, 39, L12804, doi: 10.1029/2012GL051962, 2012.

- Hsu, S. C., Tsai, F., Lin, F. J., Chen, W. N., Shiah, F. K., Huang, C., Chan, C. Y., Chen, C. C., Liu, T. H., Chen, H. Y., Tseng, C. M., Hung, G. W., Huang, C. H., Lin, S. H., Huang, Y. T.: A super Asian dust storm over the East and South China Seas: Disproportionate dust deposition, *J. Geophys. Res.*, 118(13), 7169–7183, doi: 10.1002/jgrd.50405, 2013.
- Jacobson, M. Z.: Strong radiative heating due to the mixing state of black carbon in atmospheric aerosols, *Nature*, 409, 695–697, 2001.
- Jacobson, M. Z.: Investigating cloud absorption effects: Global absorption properties of black carbon, tar balls, and soil dust in clouds and aerosols, *J. Geophys. Res.*, 117(D6), D06205, doi: 10.1029/2011JD017218, 2012.
- Kim, W., Doh, S., Yu, Y., Lee, M.: Role of Chinese wind-blown dust in enhancing environmental pollution in Metropolitan Seoul, *Environ. Pollut.*, 153, 333–341, 2008.
- 10 Kobayashi, F., Iwata, K., Maki, T., Kakikawa, M., Higashi, T., Yamada, M., Ichinose, T., Iwasaka, Y.: Evaluation of the toxicity of a Kosa (Asian dust storm) event from view of food poisoning: Observations of Kosa cloud behavior and real-time PCR analyses of Kosa bioaerosols during May 2011 in Kanazawa, Japan, *Air Quality, Atmosphere & Health*, 9(1), 3–14, 2016.
- Kimura, R.: Factors contributing to dust storms in source regions producing the yellow-sand phenomena observed in Japan from 1993 to 2002, *J. Arid Environ.*, 80, 40-44, 2012.
- 15 Watanabe, M., Yamasaki, A., Burioka, N., Kurai, J., Yoneda, K., Yoshida, A., Igishi, T., Fukuoka, Y., Nakamoto, M., Tsuchi, H., Suyama, H., Tatsukawa, T., Chikumi, H., Matsumoto, S., Sako, T., Hasegawa, Y., Okazaki, R., Harasaki, R., Horasaki, K., Shimizu, E.: Correlation between Asian Dust Storms and Worsening Asthma in Western Japan, *Allergology International*, 60, 267-275, doi: 10.2332/allergolint.10-OA-0239, 2011.
- 20 Laurent, B., Marticorena, B., Bergametti, G., Chazette, P., Maignan, F., Schmechtig, C.: Simulation of the mineral dust emission frequencies from desert areas of China and Mongolia using an aerodynamic roughness length map derived from the POLDER/ADEOS 1 surface products, *J. Geophys. Res.*, 110, D18S04, doi:10.1029/2004JD005013, 2005.
- Laurent, B., Marticorena, B., Bergametti, G., Mei, F.: Modeling mineral dust emissions from Chinese and Mongolian deserts, *Global. Planet. Change*, 52, 121–141, 2006.
- 25 Lee, K. H., Kim, Y. J., Kim, M. J.: Characteristics of aerosol observed during two severe haze events over Korea in June and October 2004, *Atmos. Environ.*, 40(27), 5146–5155, 2006.
- Lee, Y. C., Yang, X., Wenig, M.: Transport of dusts from East Asian and non-East Asian sources to Hong Kong during dust storm related events 1996–2007, *Atmos. Environ.*, 44, 3728–3738, 2010.
- Lee, H., Kim, H., Honda, Y., Lim, Y. H., Yi, S.: Effect of Asian dust storms on daily mortality in seven metropolitan cities of Korea, *Atmos. Environ.*, 79, 510–517, 2013.
- 30 Lin, I. I., Chen, J. P., Wong, G. T. F., Huang, C. W., Lien, C. C.: Aerosol input to the South China Sea: results from the moderate resolution imaging spectro-radiometer, the Quick Scatterometer, and the measurements of pollution in the troposphere sensor, *Deep-Sea Res. PT. II*, 2, 1589–1601, 2007.

- Mahowald, N. M., Kloster, S., Engelstaedter, S., Moore, J. K., Mukhopadhyay, S., McConnell, J. R., Albani, S., Doney, S. C., Bhattacharya, A., Curran, M. A. J., Flanner, M. G., Hoffman, F. M., Lawrence, D. M., Kindsay, K., Mayewski, P. A., Neff, J., Rothenberg, D., Thomas, E., Thornton, P. E., Zender, C. S.: Observed 20th century desert dust variability: Impact on climate and biogeochemistry, *Atmos. chem. phys.*, 10, 10,875–10,893, 2010.
- 5 Natsagdorj, L., Jugder, D., Chung, Y. S.: Analysis of dust storms observed in Mongolia during 1937-1999, *Atmos. Environ.*, 37, 1401–1411, 2003.
- Qian, W. H., Quan, L., Shi, S.: Variations of the dust storm in China and its climatic control, *J. Climate*, 15, 1216–1229, 2002.
- Ramana, M. V., Ramanathan, V., Feng, Y., Yoon, S. C., Kim, S. W., Carmichael, G. R., Schauer, J. J.: Warming influenced  
10 by the ratio of black carbon to sulphate and the black-carbon source, *Nat. Geosci.*, 3, 542–545, 2010.
- Schepanski, K., Tegen, I., Macke, A.: Saharan dust transport and deposition towards the tropical northern Atlantic, *Atmos. chem. phys.*, 9, 1173–1189, 2009.
- Stein, A. F., Taylor, A. D.: Horizontal dispersion parameters for long-range transport modeling, *J. Appl. Meteor.*, 21, 367–372, 1982.**
- 15 Stein, A. F., Draxler, R. R., Rolph, G. D., Stunder, B. J. B., Cohen, M. D., Ngan, F.: NOAA’s HYSPLIT atmospheric transport and dispersion modeling system, *American Meteorological Society* 12, 2059–2077, doi: <http://dx.doi.org/10.1175/BAMS-D-14-00110.1>, 2015.
- Tratt, D. M., Frouin, R. J., Westphal, D. L.: April 1998 Asian dust event: A southern California perspective, *J. Geophys. Res.*, 106(D16), 18, 371–18, 379, doi:10.1029/2000JD900758, 2001.
- 20 Uno, I., Eguchi, K., Yumimoto, K., Takemura, T., Shimizu, A., Uematsu, M., Liu, Z., Wang, Z., Hara, Y., Sugimoto: Asian dust transported one full circuit around the globe, *Nat. Geosci.*, 2, 557–560, 2009.
- Wang, S., Wang, J., Zhou, Z., Shang, K.: Regional characteristics of three kinds of dust storm events in China, *Atmos. Environ.*, 39, 509–520, 2005.
- Wang, Y., Zhuang, G., Tang, W., Sun, Y., Wang, Z., An, Z.: The evolution of chemical components of aerosols at five  
25 monitoring sites of China during dust storms, *Atmos. Environ.*, 41, 1091–1106, 2007.
- Wang, Y., Wai, K. W., Gao, J., Liu, X., Wang, T., Wang, W.: The impacts of anthropogenic emissions on the precipitation chemistry at an elevated site in North-eastern China, *Atmos. Environ.*, 42, 2959–2970, 2008.
- Watanabe, M., Yamasaki, A., Burioka, N., Kurai, J., Yoneda, K., Yoshida, A., Igishi, T., Fukuoka, Y., Nakamoto, M., Takeuchi, H., Suyama, H., Tatsukawa, T., Chikumi, H., Matsumoto, S., Sako, T., Hasegawa, Y., Okazaki, R.: Correlation  
30 between Asian Dust Storms worsening Asthma in western Japan. *Allergology International* 60(3), 267–275, 2011.
- Xuan, J., Skolik, I. N., Hao, J., Guo, F., Mao, H., Yang, G.: Identification and characterization of sources of atmospheric mineral dust in East Asia, *Atmos. Environ.*, 38, 6239–6252, 2004.

Yamaguchi, N., Ichijo, T., Sakotani, A., Baba, T., Nasu, M.: Global dispersion of bacterial cells on Asian dust, *Scientific Reports*, 2(525), doi:10.1038/srep00525, 2012.

Yang, K.L.: Spatial and seasonal variation of PM10 mass concentrations in Taiwan, *Atmos. Environ.*, 36, 21, 3403-3411, 2002.

5 Yumimoto, K., Eguchi, K., Uno, I., Takemura, T., Liu, Z., Shimizu, A., Sugimoto, N.: An elevated large-scale dust veil from the Taklimakan Desert: Intercontinental transport and three-dimensional structure as captured by CALIPSO and regional and global models, *Atmos. chem. phys.*, 9, 8545–8558, 2009.

Zhao, Q., He, K., Rahn, K. A., Ma, Y., Jia, Y., Yang, F., Duan, F., Lei, Y., Chen, G., Cheng, Y., Liu, H., Wang, S.: Dust storms come to Central and Southwestern China, too: implications from a major dust event in Chongqing, *Atmos. chem.*

10 *phys.*, 10, 2615–2630, 2010.

Zhang, X. Y., Gong, S. L., Zhao, T. L., Arimoto, R., Wang, Y. Q., Zhou, Z. J.: Sources of Asian dust and role of climate change versus desertification in Asian dust emission. *Geophys. Res. Lett.* 30, 2272, doi:10.1029/2003GL018206, 2003.

Zhang, Y., Chen, Z., Zhu, B., Luo, X., Guan, Y., Guo, S., Nie, Y.: Land desertification monitoring and assessment in Yulin of Northwest China using remote sensing and geographic information systems (GIS), *Environ. Monit. Assess.*, 147, 327–337,

15 2008.

**Table 1: Azimuthal dependence of ADS transport path**

	BR	DJ	KS	UR	Total
N–NW (northerly 360° to northwesterly 315°)	184	239	386	172	981
W–NW (westerly 270° to northwesterly 315°)	113	332	320	193	958
W–SW (westerly 270° to southwesterly 235°)	14	46	31	50	141
S–SW (southerly 180° to southwesterly 235°)	7	13	10	24	54
N–NE (northerly 0° to easterly 45°)	9	17	16	10	52
S–SE (southerly 180° to southeasterly 135°)	3	5	3	12	23
Unclassified (45° to 135°)	3	8	5	4	20
Total	333	660	771	465	2229

For each ADS event, backward trajectories for three different endings of altitude were traced from January 2003 to August 2015.

**Table 2: Summary of ADS discharge from January 2003 to August 2015**

	BR	DJ	KS	UR
number of days ( $n_{\text{ADS}}$ ) with advisory warning issued ADS events ( $\rho_{\text{dd}} \geq 150 \mu\text{g m}^{-3}$ )	111	220	257	155
number of days ( $n_{\text{ADS}}$ ) with danger warning issued ADS events ( $\rho_{\text{dd}} \geq 400 \mu\text{g m}^{-3}$ )	37	5	7	3
cumulative sum of dust density ( $\rho_{\text{cdd}}$ ) in ( $\mu\text{g m}^{-3}$ )	47,147	34,123	36,021	29,383
annual mean of cumulative sum of dust density in ( $\mu\text{g m}^{-3}$ )	3626.7	2624.8	2770.8	2260.2
mean dust density ( $\rho_{\text{mean}}$ ) of ADS events in ( $\mu\text{g m}^{-3}$ )	424.75	155.10	140.16	189.57
median dust density ( $\rho_{\text{median}}$ ) of ADS events in ( $\mu\text{g m}^{-3}$ )	318.72	162.13	164.49	171.62

**Table 3: Statistical significance of the increased occurrence rate of ADS events.**

Location	Interval	Years	Mean	$1 \sigma$	Welch $t$ -test	$p$
DJ	1960–2000	41	4.073	3.965	2.842	$7.611 \times 10^{-7}$
	2001–2015	15	17.200	6.461		
	1960–1997	36	3.833	3.753	2.627	$2.930 \times 10^{-7}$
	1998–2015	18	15.889	6.703		
KS	1960–2000	39	1.744	2.302	2.293	$1.389 \times 10^{-4}$
	2001–2015	15	14.267	9.392		
	1960–1997	36	1.444	2.076	2.110	$6.816 \times 10^{-5}$
	1998–2015	18	12.778	9.214		
UR	1988–2000	13	4.308	3.794	1.431	$1.987 \times 10^{-5}$
	2001–2015	15	20.867	10.453		
	1988–1997	10	3.200	2.658	1.202	$1.115 \times 10^{-5}$
	1998–2015	18	18.722	10.845		

The Welch's  $t$ -test is used to test the hypothesis that two populations have equal means. The Welch's  $t$ -test is an extension of Student's  $t$ -test and is more reliable when the two sample sets have unequal variances and unequal sample sizes. The value of "p" is the probability of obtaining significantly different sample means between two data sets.

**Table 4: Kolmogorov-Smirnov comparison of two data sets.**

	BR	DJ	KS	UR
BR	D=0.0000	D=0.6787	D=0.6316	D=0.5954
	P=1.0000	P=0.0000	P=0.0000	P=0.0000
DJ		D=0.0000	D=0.1326	D=0.1789
		P=1.0000	P=0.0280	P=0.0050
KS			D=0.0000	D=0.0707
			P=1.0000	P=0.7040
UR				D=0.0000
				P=1.0000

The maximum difference between the cumulative distribution (D) and corresponding probability (P) according to the Kolmogorov-Smirnov test.

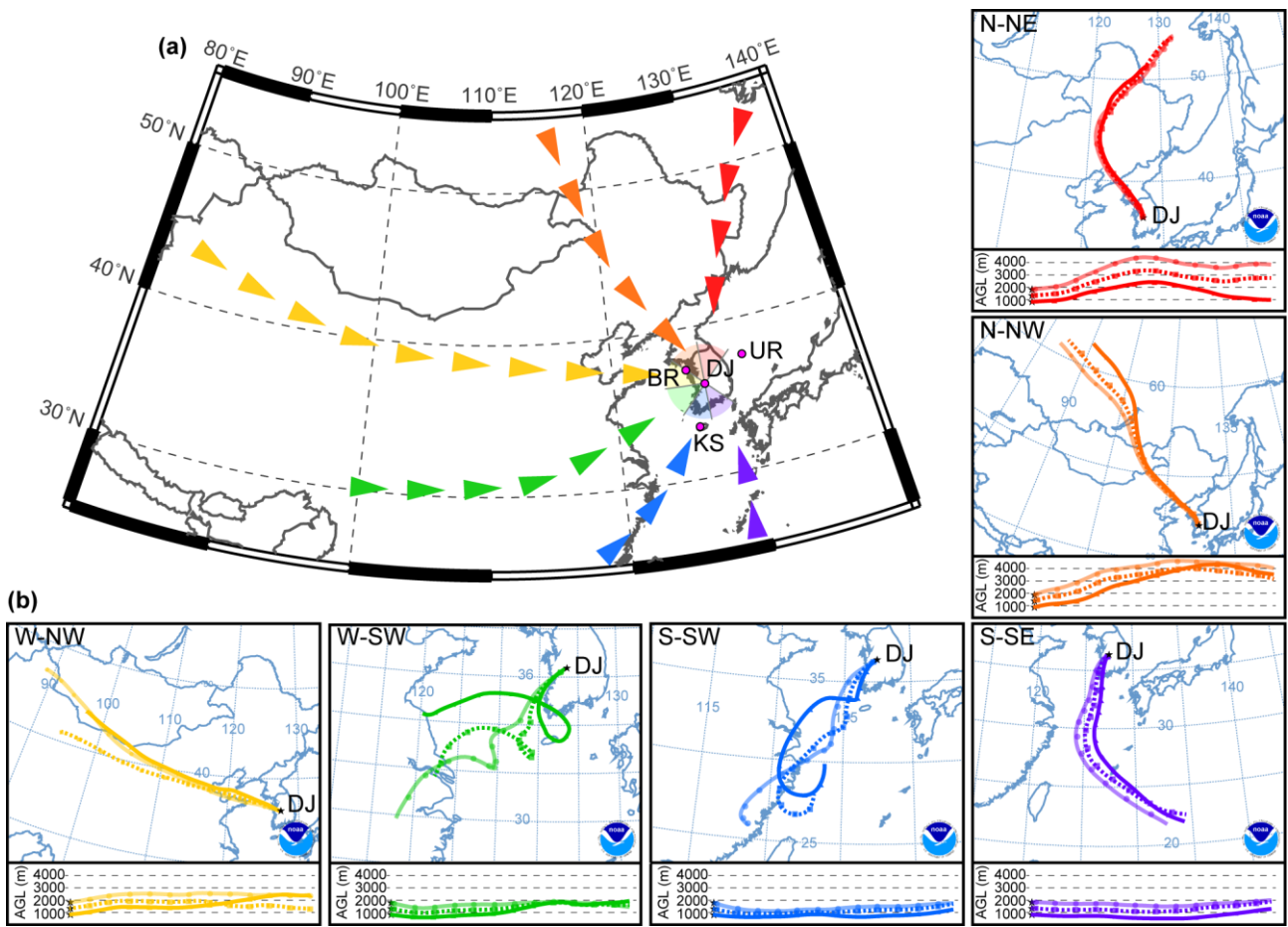
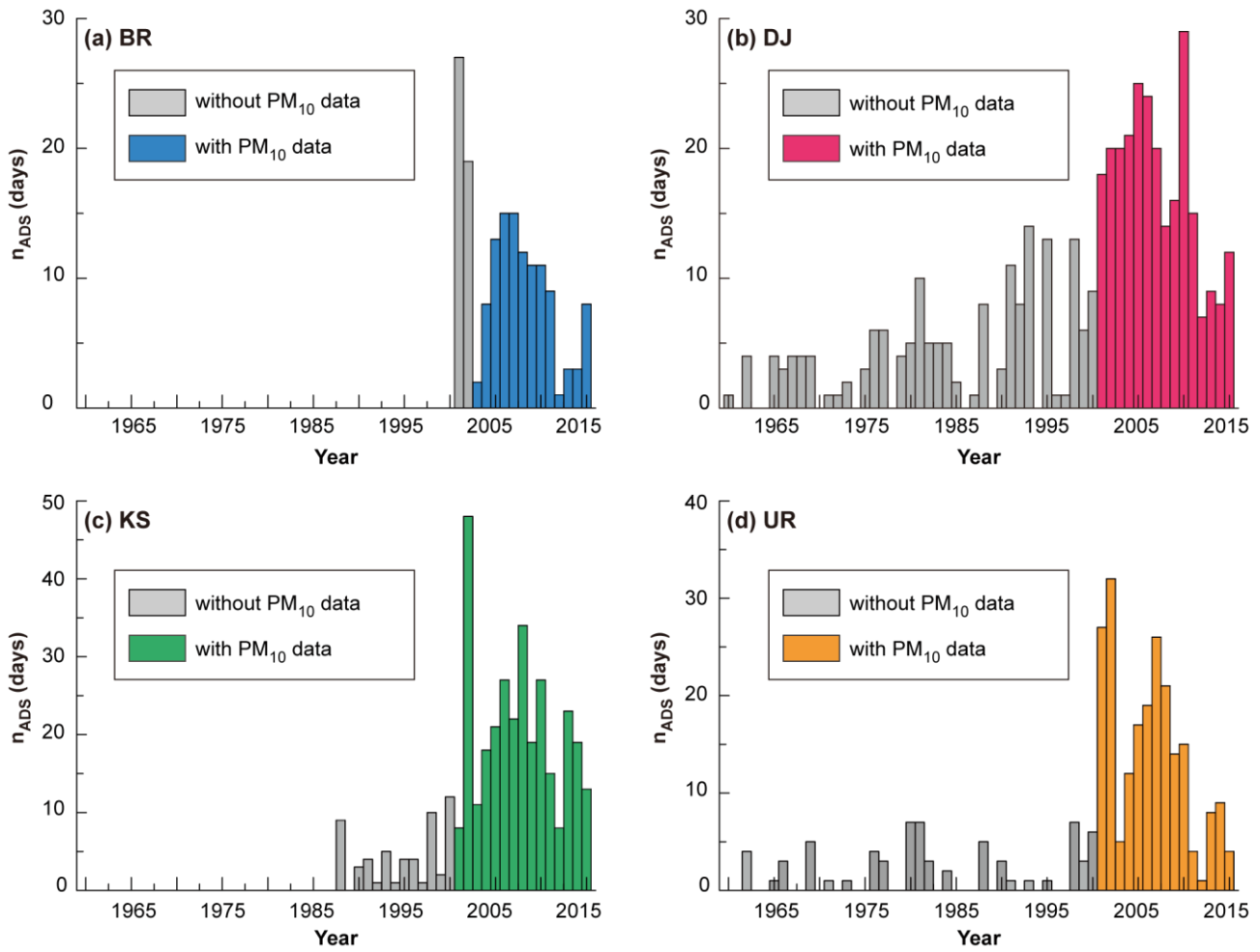
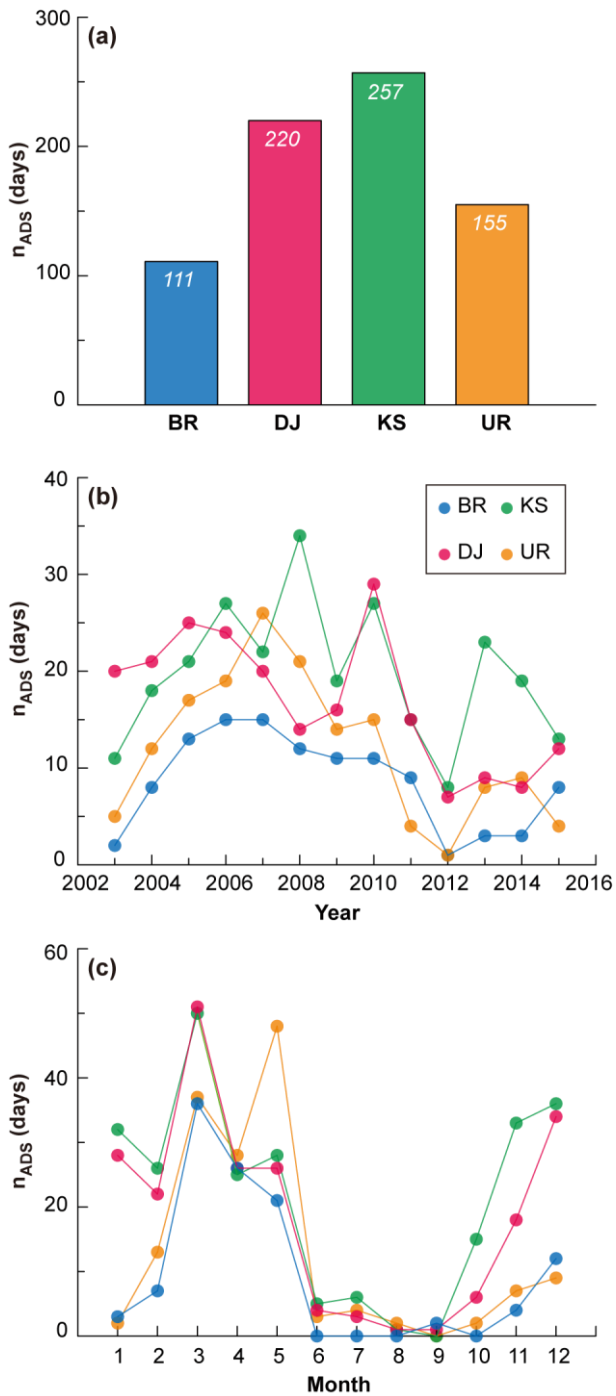


Figure 1: Figure 1: (a) Schematic diagram of dust transport path, BR: Baekryeongdo, DJ: Daejeon, KS: Kosan, UR: Ulreongdo. (b) Representative examples of HYSPLIT backward trajectories ending at DJ. Trajectories of dust transport at 1000 m, 1500 m, and 2000 m above mean sea level (AMSL) were traced for 72 hours. ADS was classified into six transport path on the basis of wind azimuth during the first 24 hours of each ADS event as N-NE (northerly 0° to northeasterly 45°), N-NW (northerly 360° to northwesterly 315°), W-NW (westerly 270° to northwesterly 315°), W-SW (westerly 270° to southwesterly 235°), S-SW (southerly 180° to southwesterly 235°), and S-SE (southerly 180° to southeasterly 135°).



**Figure 2: Number of days each year with ADS events ( $n_{\text{ADS}}$ ) at (a) BR, (b) DJ, (c) KS, (d) UR. Modern data set includes the PM<sub>10</sub> observations.**



**Figure 3: Comparison of ADS events for the past 13 years. (a) number of days each year with ADS events ( $n_{ADS}$ ) in histogram, (b) annual variations of ADS events, (c) monthly variations of ADS events.**

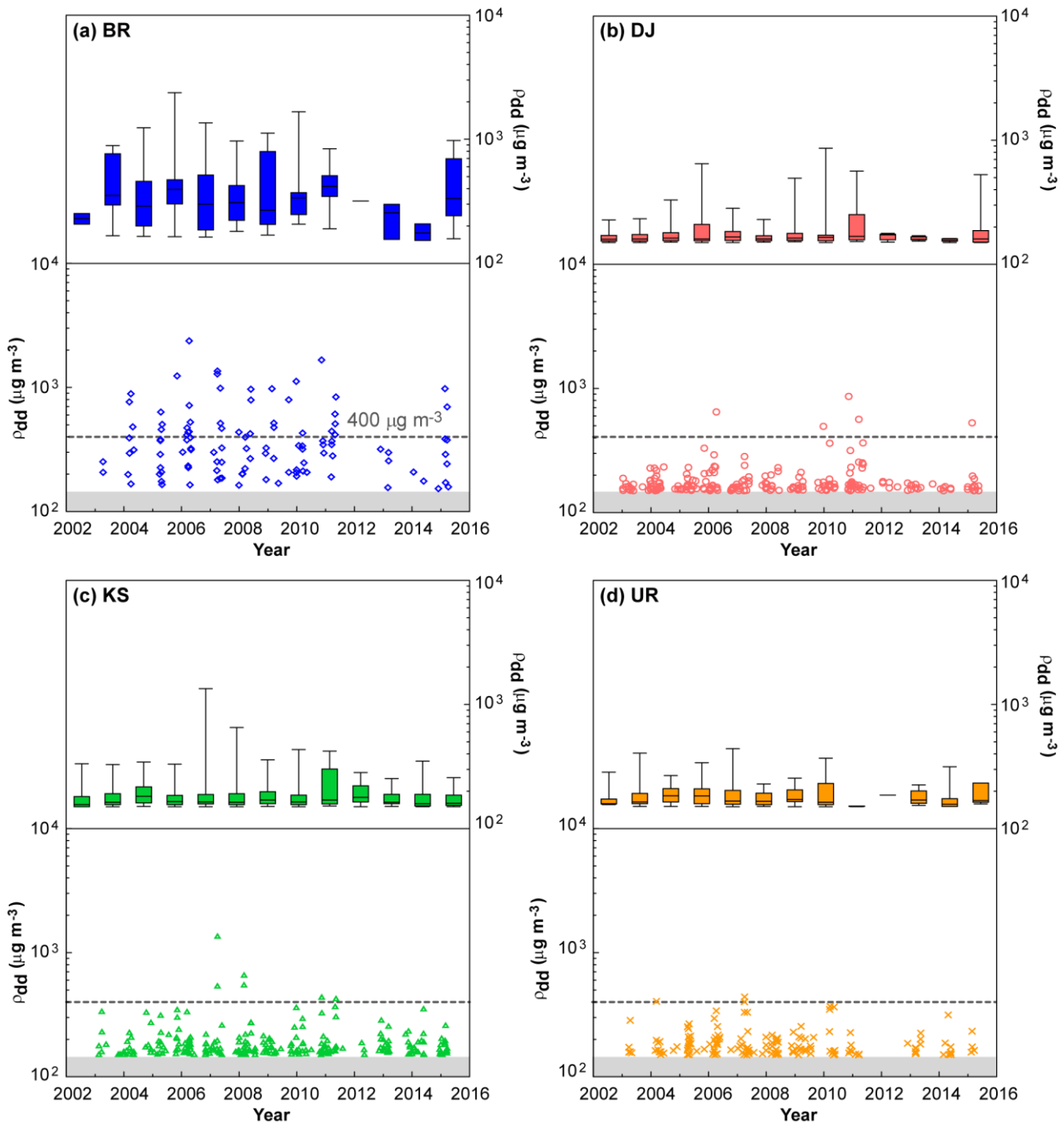


Figure 4: Annual variations of dust density ( $\rho_{ad}$ ) at (a) BR, (b) DJ, (c) KS, (d) UR. The lower panel shows a distribution of individual dust density. The upper panel displays boxplots where central box represents the inter-quartile of annual mean dust density and whisker lines are extending beyond the maximum and the minimum. In the present study, individual ADS event was accounted as the day with advisory warning with ( $\rho_{ad}$ ) exceeds  $150 \mu\text{g m}^{-3}$  for an hour. Another reference line for more significant danger warning with ( $\rho_{ad}$ ) exceeds  $400 \mu\text{g m}^{-3}$  for an hour was marked for comparison.

5

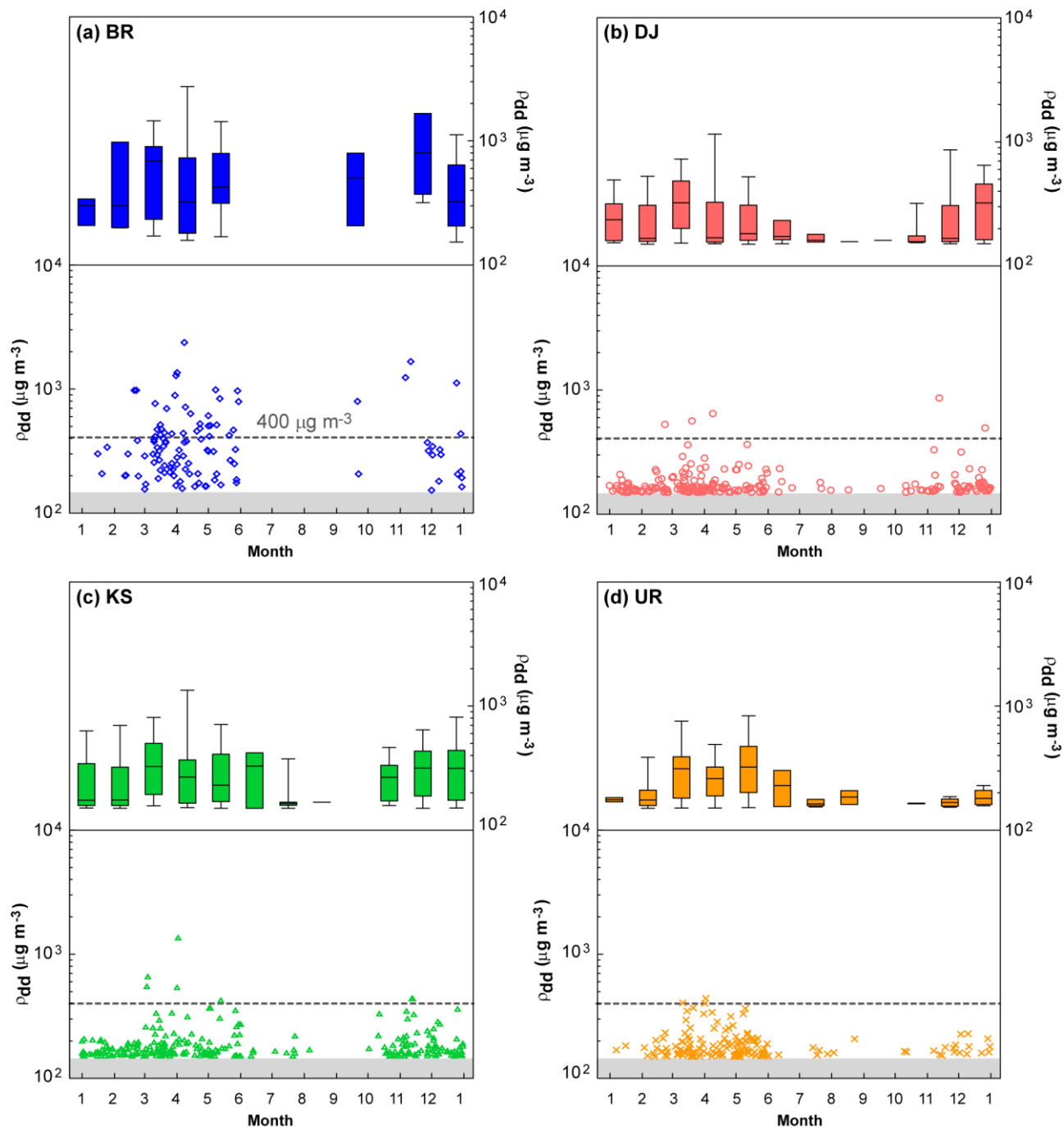
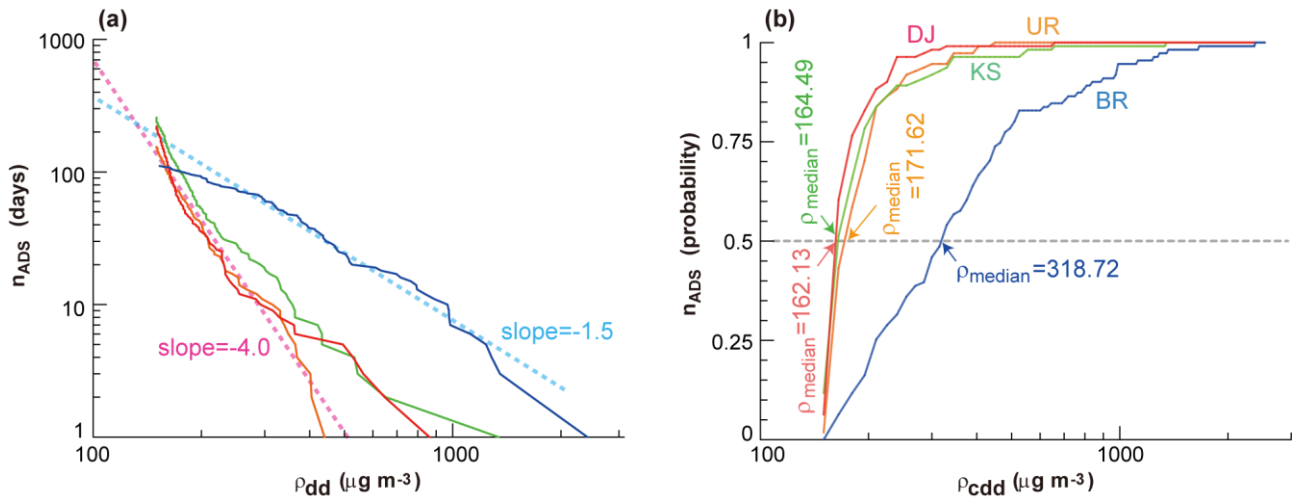


Figure 5: Monthly variations of dust density ( $\rho_{Dd}$ ) at (a) BR, (b) DJ, (c) KS, (d) UR. The lower panel shows a distribution of individual dust density. Data symbols and reference lines are as in Fig. 4.



**Figure 6:** (a) Power-law fit to the ADS events as a function of dust density ( $\rho_{dd}$ ). The two reference lines are  $(n_{ADS}) \propto (\rho_{dd})^{-1.5}$  and  $(n_{ADS}) \propto (\rho_{dd})^{-4.0}$ . (b) Cumulative distribution functions for the ADS data. Median values of dust densities ( $\rho_{median}$ ) were  $318.72 \mu\text{g m}^{-3}$  for BR,  $162.13 \mu\text{g m}^{-3}$  for DJ,  $164.49 \mu\text{g m}^{-3}$  for KS, and  $171.62 \mu\text{g m}^{-3}$  for UR.

5

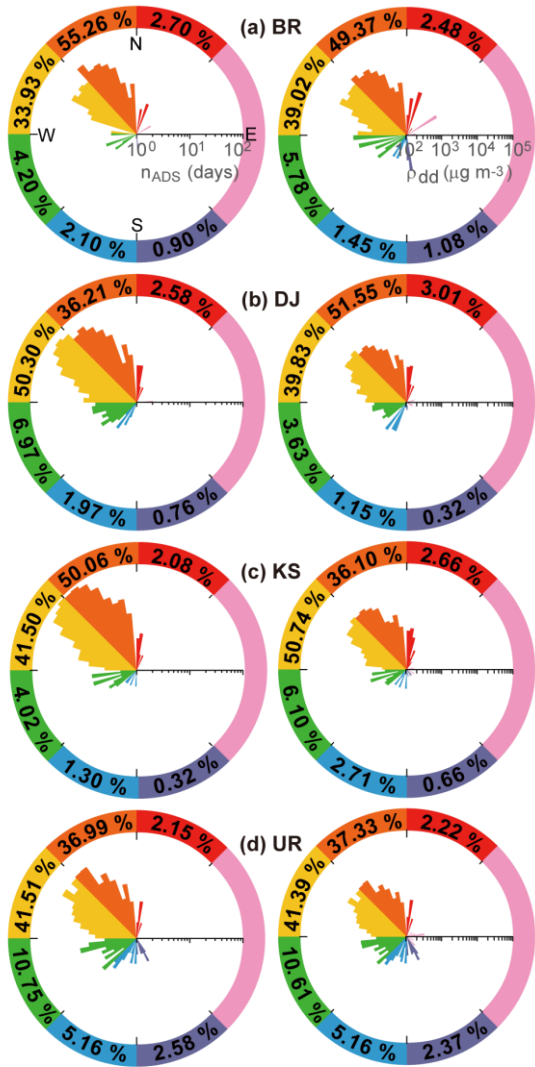
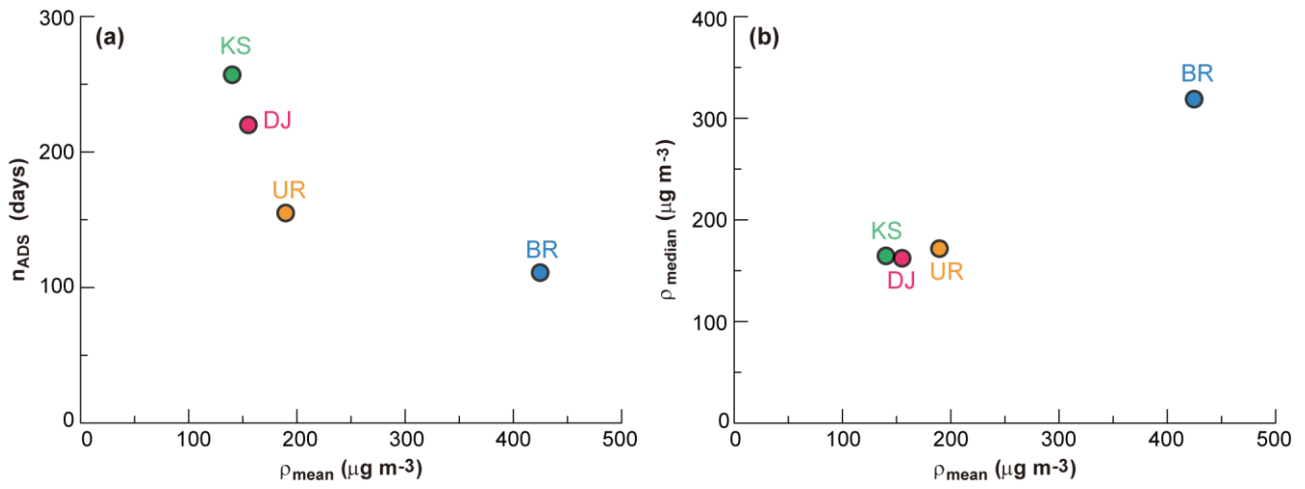


Figure 7: Spatial distribution of ADS on a Rose diagram for (a) BR, (b) DJ, (c) KS, (d) UR. The left panel shows an angular distribution of number of days each year with ADS events ( $n_{ADS}$ ). The right panel shows an angular distribution of dust densities ( $\rho_{dd}$ ).



**Figure 8: (a) An inverse correlation between ( $n_{\text{ADS}}$ ) and annual mean dust densities ( $\rho_{\text{mean}}$ ). (b) A positive correlation between median dust densities ( $\rho_{\text{median}}$ ) and annual mean dust densities ( $\rho_{\text{mean}}$ ).**